Deposition Area, Growth Rate, and Arc Power Scaling Laws for Diamond Film Deposited by Arc-Heated Gas Flows

Robert M. Young

Westinghouse Electric Corporation
Science & Technology Center
1310 Beulah Road
Pittsburgh, PA 15235 USA

I. ABSTRACT

A one-dimensional theoretical analysis, based on the convective heat transfer and convective mass transfer analogy, is given deriving scaling law relationships between thin film diamond deposition rate (grams/hour and mm/hour), target diameter (meters), and arc-heater electrical power (kilowatts). It is found that the arc-heater power is directly linear with the total deposition rate (grams/hour), and that both of these quantities increase more than linearly with target radius going as $R^{3/2}$, while the average thickness deposition rate (mm/hour) decreases as $R^{-1/2}$. Finally, experimental data taken from two Westinghouse reactors are shown on plots of deposition rate and arc-heater power vs. substrate radius, with reasonable agreement between theory and experiment.

II. INTRODUCTION

As chemical vapor deposition (CVD) of diamond films becomes an industrially useful process, scaling laws and design rules are needed to provide optimized deposition parameters. Some arc-heater scaling laws have already been put forward by Goodwin [1] for pure hydrogen arc-heated diamond CVD, using a model linking diamond growth to gas velocity and system pressure. Optimal conditions for rapid growth of high quality diamond were found to be at velocities near that of sonic (Mach number = 1) and at pressures around 1 atmosphere. In the analysis that follows, we will establish scaling laws linking arc-heater power, target diameter, and film growth rates.

III. THEORY

The heat/mass transfer analogy will be used to generate the desired scaling laws. In a DC arc-jet CVD diamond reactor (Fig. 1), a hydrogen/argon mixture is heated by passing the gas flow through an arc-heater. A small amount (c. 1%) of carbon feedstock (usually methane) along with other trace gases (e.g. oxygen) is also introduced into the jet. The hot jet impinges upon a substrate held at a temperature in the neighborhood of 1200K. More details may be found in References 5, 6, and 7.

This flow is modeled as that near an axially symmetric stagnation point. To make the problem amenable to one-dimensional analysis, the flowfield is assumed to be uniform. (In the real reactor the jet issues from an orifice much smaller than the target

diameter and spreads out before stagnating against the target. Pitot probe velocity head measurements have shown that the resulting jet is peaked at the center, and falls off radially [7].) Likewise, for the convenience of an analytical solution, the thermodynamic and transport properties will be used at a constant average value.

The dimensionless flow parameter Re (Reynolds number) is related to the dimensionless local heat transfer parameter Nu (Nusselt number) by [2,3]:

$$Nu/(Re^{1/2}) = (hr/k)/((rUr/\mu)^{1/2}) = c_1 \qquad \text{Eq. 1}$$

where c_1 is a constant. This means that the local heat flux q" (W/m^2) can be written as:

$$q" = h(T_\infty - T_W) = c_1 k(T_\infty - T_W)\,((\rho U/\mu)^{1/2})\,(r^{-1/2}). \qquad \text{Eq. 2}$$

This may be integrated to find the total heat load, Q_{tot} (Watts), transferred to a target of radius R:

$$Q_{tot} = \int_0^R q" \, 2\pi r dr = 2\pi\, c_1 k(T_\infty - T_W)\,((\rho U/\mu)^{1/2}) \int_0^R (r^{+1/2}) dr,$$

$$Q_{tot} = (4\pi/3)\, c_1\, k(T_\infty - T_W)\,((\rho U/\mu)^{1/2})\,(R^{+3/2}). \qquad \text{Eq. 3}$$

The analogy between convection heat transfer and convection mass transfer [4] is next used to establish a relationship to the deposition rate. The local Nusselt number is linked to the local Sherwood number Sh (the dimensionless mass transfer parameter) by the Lewis number Le.

$$Nu = (Le^{-1/3})\,Sh = ((\alpha/D)^{-1/3})\,(h_D r/D) = ((k/\rho c_p D)^{-1/3})\,(h_D r/D). \qquad \text{Eq. 4}$$

For many flows, the Lewis number Le = 1, in which case the temperature and concentration profiles coincide.

Since the local mass flux equation $m" = h_D(C_\infty - C_W)$ is mathematically similar to the heat transfer solution given above, we can write the total mass deposition rate M_{tot} [kg/s] on a target of radius R as:

$$M_{tot} = (4\pi/3)\, c_1\, D(C_\infty - C_W)\,((\rho U/\mu)^{1/2})\,(Le^{-1/3})\,(R^{+3/2}). \qquad \text{Eq. 5}$$

It should be noted that both the local heat flux and local mass flux equations have a singularity at r=0 (i.e. in Eq. 2 as $r \to 0$ then $q" \to \infty$) but because the integral quantities remain finite, the solution is realistic.

Finally, the total mass deposition rate can be related to the target area A (m^2) and an average thickness deposition rate t_{ave} (μm/hr):

$$M_{tot} = \rho_f t_{ave} A = \rho_f t_{ave} \pi R^2 \qquad \text{Eq. 6}$$

where ρ_f is the deposited film density, 3.52 grams/cm^3 for diamond. Equating the two expressions for M_{tot} then yields:

$$t_{ave} = (4/3\rho_f)\, c_1\, D(C_\infty - C_w)\, ((\rho U/\mu)^{1/2})\, (Le^{-1/3})\, (R^{-1/2}). \qquad \text{Eq. 7}$$

It is reasonable to assume that torch electric power is directly linear with the total heat load on the target, that is $Q_{tot} \sim Q_{torch}$. Then from the above equations, we may draw the following conclusions:

$$Q_{torch} \sim M_{tot} \sim R^{+3/2} \sim A^{+3/4}, \qquad \text{Conclusion I}$$

and

$$t_{ave} \sim R^{-1/2} \sim Q_{torch}^{-1/3}. \qquad \text{Conclusion II}$$

IV. EXPERIMENT and RESULTS

The scaling experiments reported here were conducted on two small Westinghouse reactors which are further described elsewhere [5-7]. The main difference between the two reactors is size, with the higher power machine physically larger and capable of handling larger targets. Exact parameters for the two experimental reactors are proprietary. As a public statement, we can stipulate that the four gas flows (H_2, Ar, CH_4, and O_2) were scaled linearly with the electric power. The chamber pressure was the same for both reactors, 50 Torr. The stand-off distance from the torch nozzle exit to the target was adjusted so that the same surface temperature was achieved, 894 ±15 °C (as measured by an Ircon R-16C05 two-color pyrometer). This resulted in stand-off lengths of 19 and 42 cm for the 10 and 29 kW experiments, respectively. By adjusting the stand-offs to bring the substrates to the same temperature, we match the relative heat loads on the targets, which should, by the heat/mass transfer analogy, match up the relative deposition rates.

The substrate materials were single crystal Si, with a proprietary separation/nucleation layer applied. Just prior to loading in the reactors, the samples were seeded with 1/4 micron diamond dust. While the weight gain of the smaller target was directly measurable, a scale was not available with sufficient accuracy to accommodate the weight of the larger target. Thus the weight gain was calculated from measuring the thickness profile of the deposited diamond.

The substrate diameters were chosen to scale as $R^{3/2}$ with the electric power, namely R=3.81cm (1.5") at 10 kW and R=7.62cm (3") at 29 kW. Thus the results reported here are a test as to whether the predicted dependence of the total mass deposition rate also matches this scaling. From Conclusion I above, the total mass gain

rate should show a slope of 3/2 on a log-log plot of M_{tot} vs. Q_{torch}. This is shown on the left side of Fig. 1, where the solid line has been fitted to the data, using the theoretically predicted slope of 3/2. The data lies near this solid line, however, these two points show an exact fit to a slope of 1.143. The right hand plot of Fig. 1 shows the dependence of total mass deposition rate on reactor power, with a simple linear fit to the data, also as per Conclusion I.

The mismatch of the $M_{tot} \sim R^{+3/2}$ dependency may be attributed to the many simplifying assumptions used in the development of the theory. It may also be due to experimental error, especially noting that there is only a factor of about 3 difference between these two arc-heater powers. Westinghouse is currently commissioning a 100 kW reactor, and is constructing a fourth reactor to operate at 1/2 MW. Data from these machines will provide better leverage in determination of the scaling dependency. Fig. 4 shows that for an $R^{+3/2}$ scaling, we would expect to coat disks of radius R=17.7cm (6.96") at 100 kW and R=51.7cm (20.4") at 1/2 MW. The reader should note that the thickness deposition rate (μm/hr) is predicted to fall off with increasing substrate size, as $t_{ave} \sim R^{-1/2}$. Beneficially, the total number amount of diamond (carats per hour) will always increase with radius beyond the linear due to $M_{tot} \sim R^{+1.14}$ to $R^{+3/2}$, as found from experiment and theory, respectively. Finally, the above facts also directly impact production costs. Our current economic model [5] predicts diamond production with gas recycling at a cost of under $5/ct at 100 kW. To go significantly below this cost will require even larger torches.

V. ACKNOWLEDGMENT

This work has been supported in part by the National Institute of Standards and Technology under the Advanced Technologies Program, grant no. 70NANB3H1350, and by the SGS Tool Company and the Westinghouse Electric Corporation. The advice of Drs. W.D. Partlow and J.J. Schreurs, and the assistance of Messrs. R. Hilgert and R. Roney are gratefully acknowledged.

VI. NOMENCLATURE

A = total target area coated by diamond, m^2.
c_1 = constant defined in Eq. 1, dimensionless.
c_p = gas heat capacity at constant pressure, J/kgK.
C_∞ = freestream gas phase concentration of carbon species, kg/m^3.
C_w = target surface gas phase concentration of carbon species, kg/m^3.
D = diffusion coefficient, m^2/s.
h = heat transfer coefficient, W/m^2K.
h_D = mass transfer coefficient, m/s.
k = gas thermal conductivity, W/mK.
Le = Lewis number, dimensionless.
m" = local mass transfer flux to the target, kg/m^2s.

M_{tot} = mass transfer rate to the entire target, kg/s.
Nu = Nusselt number, dimensionless.
q" = local heat flux to the target, W/m^2.
Q_{torch} = electric power input to the arc-heater, W.
Q_{tot} = heat transfer rate to the entire target, W.
r = local radial coordinate, m.
R = target outer radius, m.
Re = Reynolds number, dimensionless.
Sh = Sherwood number, dimensionless.
T_∞ = freestream gas temperature, K.
T_W = target surface temperature, K.
tave = thickness deposition rate, averaged over the target, m/s.
U = freestream gas velocity, m/s.
α = gas thermal diffusivity, m^2/s.
μ = gas viscosity, kg/ms.
ρ = gas density, kg/m^3
ρ_f = diamond density, kg/m^3

VII. REFERENCES

1. D.G. Goodwin, "Scaling Laws for Diamond Chemical-Vapor Deposition," Journal of Applied Physics, 74(11) 6888-6906 (1993).
2. J.A. Fay and N.H. Kemp, "Theory of Stagnation-Point Heat Transfer in a Partially Ionized Diatomic Gas," AIAA J. 1(12) 2741-2751 (1963).
3. E.R.G. Eckert and E. Pfender, "Advances in Plasma Heat Transfer," in *Advances in Heat Transfer, Vol. 4,* J.P. Hartnett and T.F. Irvine, Jr., Eds. (Academic Press, New York: 1967) pp.229-316.
4. J.P. Holman, *Heat Transfer, Fourth Ed.,* (McGraw-Hill Book Company, New York: 1963) p.439.
5. W.D. Partlow, J. Schreurs, R.M. Young, I. Matorell, S.V. Dighe, G.S. Swartzbeck, and J. Burton, "Low Cost Diamond Production with Large Plasma Torches," Applied Diamond Conference 1995, International Conference on the Applications of Diamond Film and Related Materials (NIST, Gaithersburg, MD 21-24 Aug. 1995).
6. R.M. Young, "Hydrogen/rare-gas optimization by simple boundary layer theory for diamond film deposition in arc-heated gas flows," Surface and Coatings Technology, 68/69, 384-387 (1994).
7. Robert M. Young and Jan J. Schreurs, "Evidence of Supersonic Flow in an Arc-Heated Diamond Film Deposition Reactor," *in preparation.*

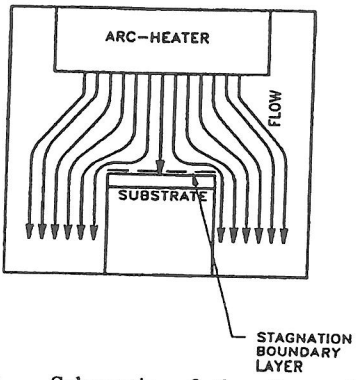

Fig. 1. Schematic of the diamond deposition process. *The arc-heater produces a hot gas flow containing monatomic hydrogen and carbon-bearing species. This flow then impinges on the substrate forming a stagnation boundary layer.*

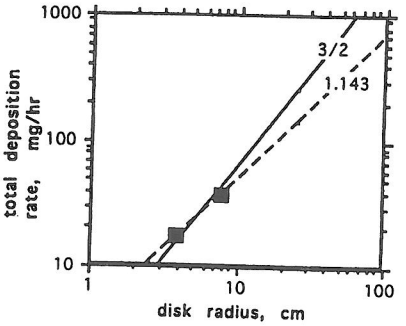

Fig. 2. Plot of total mass deposition rate vs. disk radius. *Theory predicts a slope of 3/2 on this log-log plot, as per Conclusion I:* $M_{tot} \sim R^{+3/2}$.

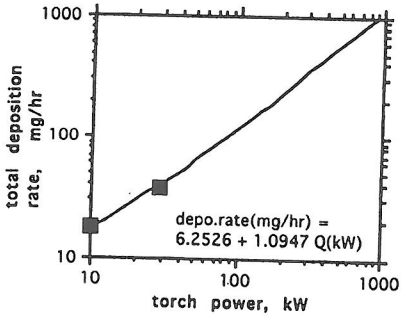

Fig. 3. Plot of total mass deposition rate vs. electric arc-heater power. *A simple linear dependence has been used to fit the data, as per Conclusion I in the text:* $Q_{torch} \sim M_{tot}$.

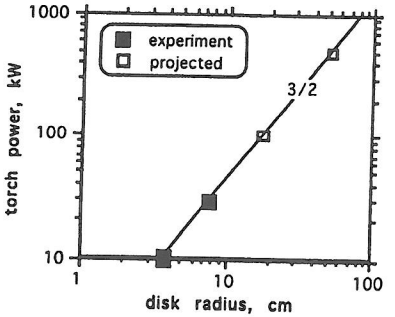

Fig. 4. Plot of required torch electric power vs. substrate radius. *This shows that for an* $R^{+3/2}$ *scaling, we would expect to coat disks of radius R=17.7cm (6.96") at 100 kW and R=51.7cm (20.4") at 1/2 MW*